Research Article
Effect of Carbide Particles on the Behaviour of the Oxide Layer

[1]Wan Fathul Hakim W. Zamri, [2]B. Kosasih, [2]K. Tieu, [1]Wan Aizon Wan Ghopa, [3]M. Faiz Md Din,
[1]Ahmad Muhammad Aziz and [1]Siti Fatimah Hassan
[1]Department of Mechanical and Materials, Faculty of Engineering and Built Environment, Universiti
Kebangsaan Malaysia, Malaysia
[2]Faculty of Engineering, University of Wollongong, Australia
[3]Faculty of Engineering, Universiti Pertahanan Nasional Malaysia, Malaysia

Abstract: In this study, an FE simulation was used to simulate the contact established between a High-Speed Steel (HSS) work roll and a hot strip material in hot rolling, in which the top layer and the substrate represented the HSS roll and the tip of the indenter represented a particle from oxide scale formed on the strip steel. As the oxidation behaviour of carbides affects the homogeneity of the oxidised surface of work rolls, this has an important influence on wear and therefore it is instructive to investigate the effect that carbide particles have on the behaviour of the oxide layer. This study focused on the interaction between the carbide and the asperity by an abrasive. The evolution of strain fields during the simulation tests was recorded at room and high temperature. The 3D FE model was able to show the interaction between the indenter and the carbide particle reinforcements of these following scenarios: particles above, along and below the scratch path. The results indicated that the strain at high temperature is higher than at room temperature which leads to a higher sensitivity to failure. Increasing the strain means high probability of particle movement that produces delamination of the layer. The strains for particles on the oxide-substrate interface at both temperatures are higher than the particle in the substrate. The interaction between the tip and the particle significantly influences the strains.

Keywords: Finite element method, high speed steel, oxide layer, particle, scratch, wear

INTRODUCTION

The existence of carbides in HSS material can influence the contact friction and wear of the oxide layer. Because carbides are much harder than the matrix they contribute to the mechanical strength, load bearing capacity and wear resistance (Park *et al*., 1999; Badisch and Mitterer, 2003). There are many carbides factors that are related to variations in the wear resistance such as the content of carbon and chromium and the fraction, size and distribution of carbide, etc. Kang *et al.* (2001) found that the wear resistance of high speed steel rolls increases with the increase of the total fraction of carbide because of increased carbon content. The authors also indicated that the wear resistance of HSS work roll improves with a smaller amount of chromium because it results in the formation of a number of very hard MC carbides. Rodenburg and Rainforth (2007) found that carbide size distribution is a major controlling factor in the mild oxidational wear of high speed steel. A reduction in the size of carbide for a constant volume fraction lowers the matrix being exposed to contact damage by decreasing the mean distance between the carbides.

Carbide precipitates in high speed steel due to the high vanadium content of these alloys (Boccalini and Sinatora, 2002). HSS work rolls consist of complex multi-component alloys. The main alloying elements in HSS are carbon, vanadium, chromium, tungsten and molybdenum. The typical microstructure of HSS consists of primary carbides (10-20%) distributed in a matrix of tempered martensite and fine secondary carbides formed from the high concentration of strong carbide forming elements such as V, W and Mo. Boccalini and Sinatora (2002) reported that an increasing amount of vanadium causes the formation of MC eutectic with an intercellular network of M_2C or M_7C_3 carbides that have a tendency to micro-spalling and subsequent falling off. As the oxidation behaviour of carbides affects the homogeneity of the oxidised surface of work rolls, this has an important influence on wear and therefore it is instructive to investigate the effect that carbide particles have on the behaviour of the oxide layer.

Corresponding Author: Wan Fathul Hakim W. Zamri, Department of Mechanical and Materials, Faculty of Engineering and Built Environment, Universiti Kebangsaan Malaysia, Malaysia

In this study, the interaction between the carbide and the asperity by an abrasive mechanism is investigated. The abrasive factor in the hot strip mill is given by asperities where the oxide layers of strips as multiple asperities and abrade the oxide layers of the work rolls. In order to work out how carbide affects the behaviour of the oxide layer, a 3D FE model was established to analyse the deformation of the oxide layers and the indenter-carbide particle interactions during a scratch process. The 3D FE model was able to show the interaction between the indenter and the carbide particle reinforcements of these following scenarios: particles above, along and below the scratch path. The development of stress and strain fields in the oxides and high speed steel substrate was analysed and physical phenomena such as removal materials, particle de-bonding and material displacement were explored. The model developed here represents an incremental advancement of the scratching FE models that explain the failure modes and mechanisms of the oxide layer on High Speed Steel (HSS).

METHODOLOGY

In the present investigation the interaction between the scratch tip and particle was categorised into 3 scenarios: particle above the scratching path, particle along the scratching path and particle below the scratching path. All three cases were chosen based on the three different possibilities of particle location which (Fig. 1) are:

- On oxide free surface
- On oxide-substrate interface
- Below oxide-substrate interface (in the substrate)

Since in the real case of HSS the carbide particles are only precipitated in the oxide-substrate interface (case b), or in the substrate (case c), as reported by

Boccalini and Sinatora (2002), Zhu *et al*. (2010) and Zamri *et al*. (2013), these two cases were analysed in next section. For case (a), which is particle located on oxide free surface, the simulation is not explained in this study since the location of the is not real.

Two cases of temperature occurred during the scratching tests: low temperature (room temperature) and high temperature (600°C). The model only considered one sub-layer due to the large 1:4 ratio of the outer sub-layer and inner layer sub-layer. During the scratch test a particle will probably go into the chip, some will be de-bonded and fractured and the remainder will probably remain on the HSS substrate.

A three dimensional finite element model was constructed using the explicit finite element method. In accordance with practice the particle was assumed to have a diameter 10 μm. This is an agreement with the size of primary M_6C and MC carbide particles reported by Vardavoulias (1994) where the particles vary between 2 and 10 μm. The assumptions and parameters used in the FE modelling are summarised in Table 1.

A three dimensional finite element model was constructed using the explicit finite element software package ANSYS/LS-DYNA version 13. The geometry of the scratch is shown in Fig. 2. The particle was assumed to be perfectly bonded, which is similar to the work reported by Pramanik *et al*. (2007). In this case the interface nodes of the matrix and particle were tied together by an interface zone. Since the interface zone is very hard and brittle and hence similar to the particles, the interface was considered to be an extension of the particle. The indenter was treated as a rigid body and moved horizontally in the oxide scale. The substrate was fully fixed on its bottom surface to eliminate rigid body motion.

The oxide scale material was a Fe_3O_4 reinforced with a carbide particle that was surrounded by an interface zone. The substrate is High Speed Steel (HSS). A plastic kinematic material and associative
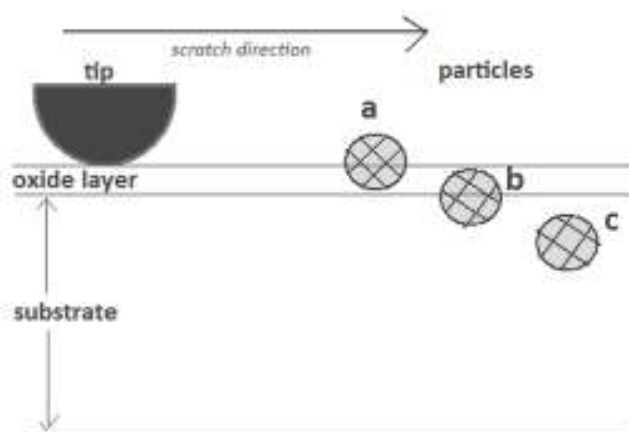

Fig. 1: Particle locations with the respect to the oxide layer; (a) particle on oxide free surface, (b) particle on oxide-substrate interface; (c): particle below oxide-substrate interface (in the substrate)
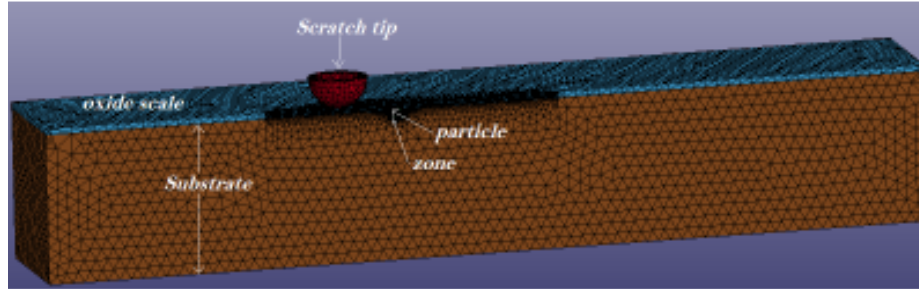
Fig. 2: 3D FE model for simulating the scratch test

Table 1: Assumptions and parameters for FEM of scratch test

Scratch depth (µm)		3.2
Outer radius zone (µm)		5.1
Inner radius particle (µm)		5
Centre point of particle (um):	a	(x, y= 40, 4)
Centre point of particle (um):	b	(x, y= 40, 2.8)
Centre point of particle (um):	c	(x, y= 40, -3.2)
Centre point of particle (um):	d	(x, y= 40, -6.2)
Centre point of particle (um):	e	(x, y= 40, 4)

Table 2: Assumptions and parameters for FEM–based scratch test modelling for ductile model

Oxide scale surface	Smooth
Oxide scale/ Substrate interface	Perfectly bonded
Scratch distance (µm)	~200
Indenter tip radius (µm)	20
Oxide scale thickness (µm)	4
Oxide scale material	Fe_3O_4
Oxide scale material properties at room temperature	E = 245 GPa, υ= 0.2, σ_y= 7 GPa
Oxide scale material properties at high temperature (600ºC)	E = 221 GPa, υ= 0.19, σ_y= 5 GPa
Substrate material properties	E = 210 GPa, υ = 0.3, σ_y= 2 GPa
Particle properties	E = 345.1 GPa, υ = 0.3

flow rule were used for the interface zone respectively. The strain rate was accounted for by using the Cowper-Symonds model which scaled the yield stress by a strain rate dependent factor and the equation to calculate yields stress in plastic kinematic material model is given below:

$$\sigma_y = \left[1 + \left(\frac{\dot{\varepsilon}}{C}\right)^{\frac{1}{P}}\right](\sigma_o + \beta E_p \varepsilon_p^{eff}) \qquad (1)$$

$$E_p = \frac{E_{tan}E}{E-E_{tan}}\pi r^2 \qquad (2)$$

where σ_y is the yield stress, σ_o is the initial yield stress, $\dot{\varepsilon}$ is the strain rates, C and P are the Cowper-Symonds strain rate parameters, ε_{eff} is the effective plastic strain, β is the hardening parameter and E_p is the plastic hardening modulus, E_{tan}, is the tangent modulus and E is the modulus of elasticity. The material properties of the oxide layer were based on the experimental results from Zamri *et al.* (2012). The two sets of mechanical properties which correspond to room temperature and high temperature were applied to the model.

A failure separation criterion available in ANSYS/LS-DYNA for this material model was used in the simulation. According to this criterion, failure separation occurs when the strain energy release rate is exceeded a critical value. During the scratch test, a cohesive zone surrounding the particle will probably go into the chip, some will be de-bonded and fractured and the rest will probably remain on the HSS substrate. In the present investigation, the interaction between the scratch tip and particle was investigated following 2 scenarios: particle on oxide-substrate interface and particle in the substrate. The consideration of the particle in both positions was based on the actual carbides where they are embedded into the oxide layer and substrate. The model of the oxide layers in this chapter was considered to be a ductile model. In this finding the behaviour of the oxide layers was confirmed to be ductile, which corresponds to their failure characteristic. The assumptions and parameters used in the FE modelling are summarised in Table 2. The model has considered one sub-layer only due to the large 1:4 ratio of the outer sub-layer and inner sub-layer.

RESULTS AND DISCUSSION

The behaviour of the oxide layer and carbide particle was investigated in terms of the strain field contour. Strain is a description of deformation in terms of relative displacement, but it also becomes an indicator to identify the failure of the element when the strain is greater 1.

The plastic strain contour has clearly increased as the scratch tip moves into the oxide layer during nanoindentation. A high distribution of the plastic strain
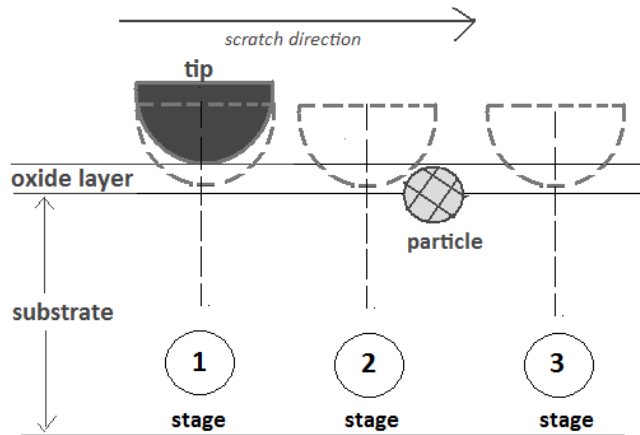
Fig. 3: Particle locations on oxide-substrate interface (Case b)

contour occurred at the interface zone of the particle when the scratch tip and the particle came into contact. Plastic deformation occurred as the oxide layer material entered into the deformation zone. Contact interaction between the scratch tip and particles caused the particles to de-bond.

There are two ways particle can de-bond, either partially or completely. De-bonding leads to particle failure during scratching. The partial de-bonding of the interface zone may cause the particles to become embedded into the oxide layer while the complete de-bonded zone may cause the particles to be removed from the oxide layer. Thus, the evolutions of strain at room temperature and high temperature leading to particle de-bonding are explained in the following section. Two cases were considered:
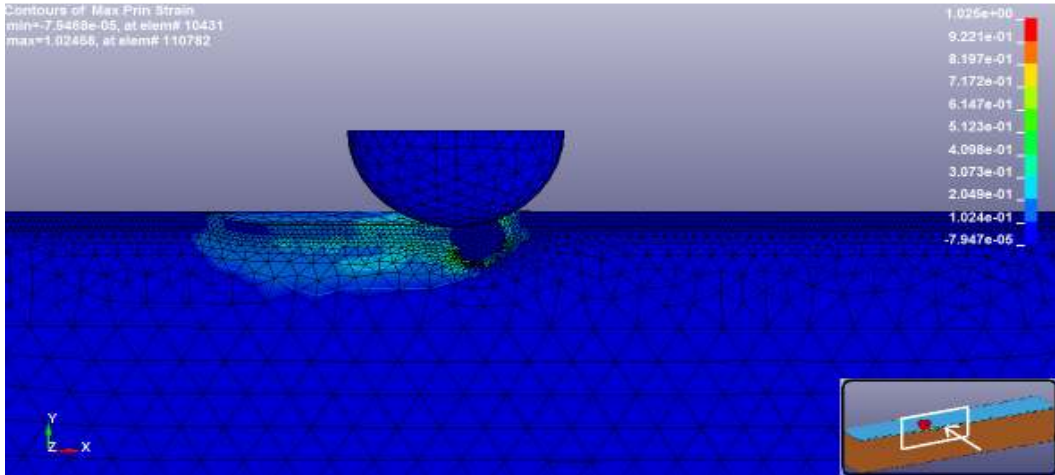
- Particle on oxide substrate interface
- Particle below oxide-substrate interface (in the substrate)

Particle on oxide substrate interface: The evolution of strain fields during scratching for a particle located on the oxide-substrate interface was analysed in 3 stages; after nanoindentation, during tip-particle contact and post tip-particle contact (Fig. 3). Initially the tip indents on the oxide layer and substrate (stage 1 in Fig. 3), then interacts with the particle at the scratching edge (stage 2 in Fig. 3) and then continues to move until the scratching process ends (stage 3 in Fig. 3).

Figure 4 shows the simulation at room temperature strain field result while Fig. 5 is the result from simulation at high temperature (600°C) for the three consecutive stages of the scratching process. The strain contours after nanoindentations are shown in Fig. 4a and 5a. The compressive and tensile strains are perpendicular to the scratch tip during nanoindentation into the oxide layer and substrate.

As can be seen from Fig. 4a and 5a, the maximum strain is up to 0.02, after which it then slides into
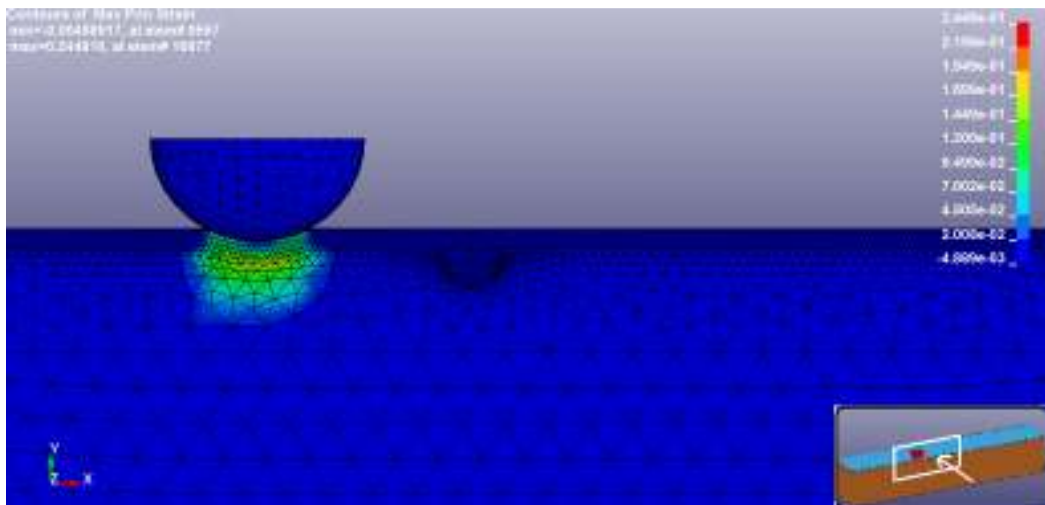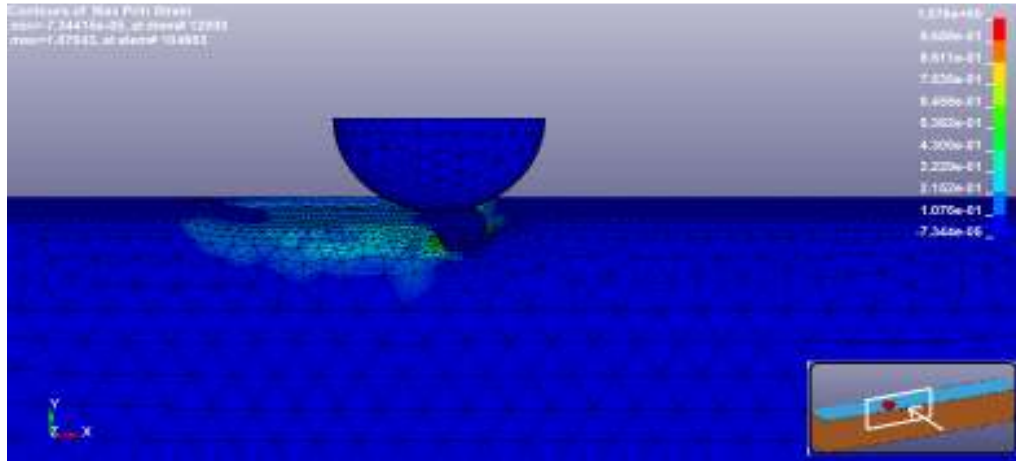

(a)
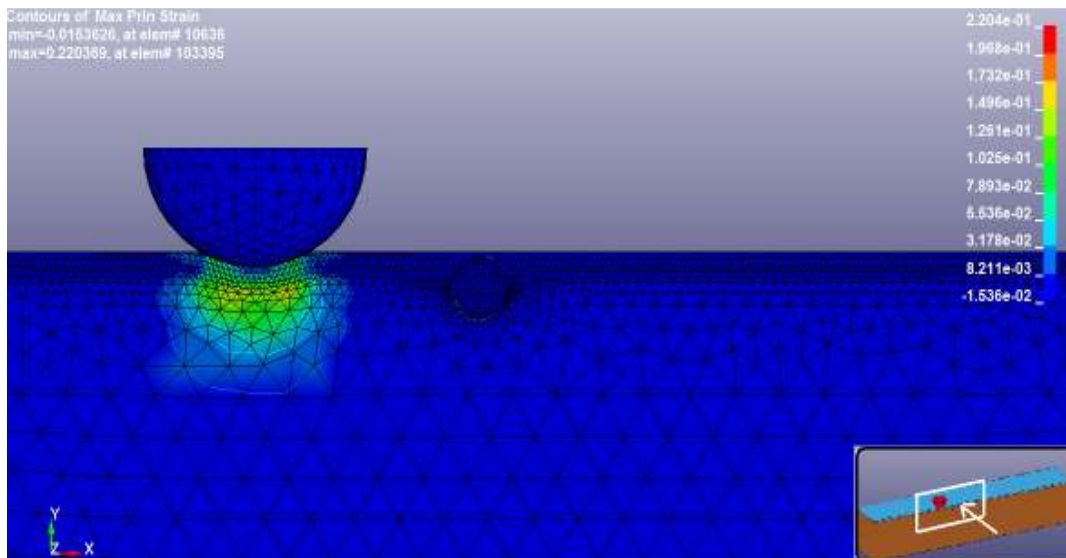
(b)
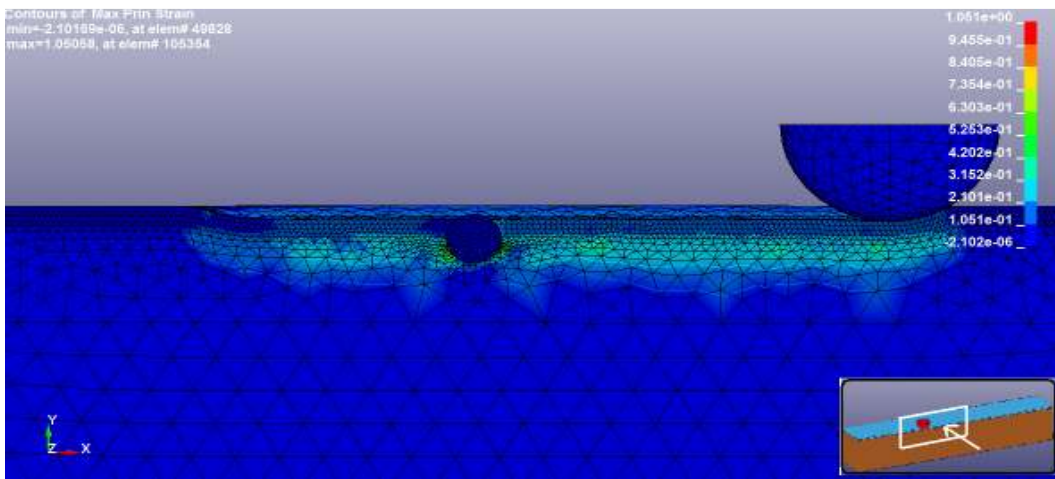
(c)

Fig. 4: The strain field of the particle on oxide substrate interface at room temperature; (a) before scratching, (b) during scratching, (c) after scratching
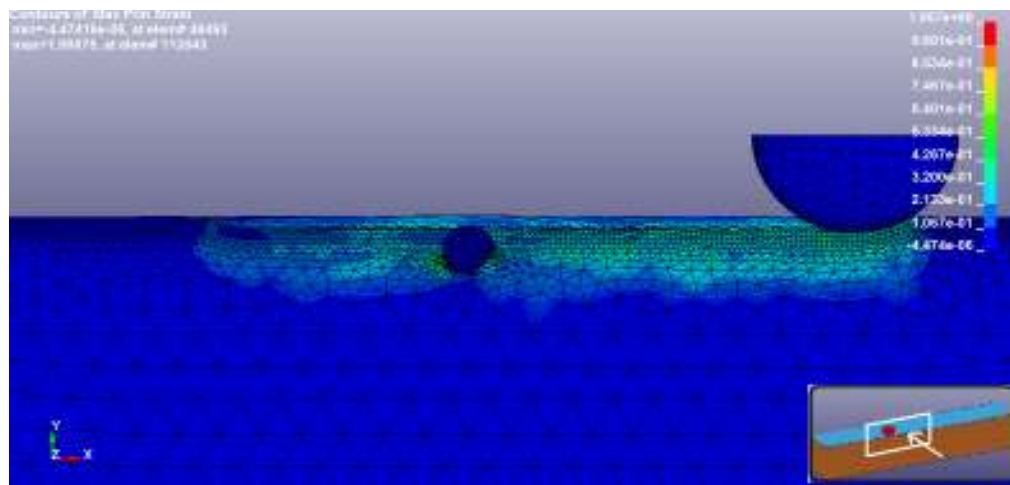

(a)

(b)

(c)

Fig. 5: The strain field of the particle on oxide substrate interface at high temperature; (a) before scratching, (b) during scratching, (c) after scratching

the oxide scale layer causing a high plastic strain in the surrounding oxide and substrate (stage 2). As scratching progresses the particle is partially de-bonded after the tip and the particle interact at the edge of the scratching (Fig. 4b and 5b). Both cases (low and high temperature) showed the maximum strain contour beyond the strain limit which were 1.025 (Fig. 4b) and 1.07 (Fig. 4b) respectively.

Since the maximum strain was slightly higher than the strain limit (strain limit = 1), the fragment of the interface zone was not too significant so as a result, the movement of the particle was not too obvious. This situation might be related to the attack angle between the scratch tip and particle. As the tip moved further (stage 3), the particle moved slightly forward (Fig. 4c and 5c). The movement of slider lead to the particle appearing at the surface due to fracture at the bonding interface between the particle and oxide layer. At this stage the contours section had the higher strain of 1.05

compared to stage 2 at room temperature, as shown in Fig. 4. This condition might be due to particles on the lower part of cutting edge becoming de-bonded, leading to an increase in the strain.

Comparing the strain obtained from room temperature (Fig. 4) and high temperature (Fig. 5), maximum strain at high temperature was higher than at a low temperature. This situation was probably influenced by the mechanical properties of the oxide layer and carbide. The lower elastic modulus and yield strength of oxide scale at high temperature influenced the higher strain result of oxide scale and particles. If the material has a high elastic modulus, it takes higher load for the shape to deform. In other words, the high potential for abrasive wear is given by the oxide layer formed on high speed steel at high temperature.

Particle below the oxide-substrate interface (in the substrate): The orientation between the tip and the

particle was categorised under this case if the particle is situated below the oxide-substrate interface (Fig. 6).

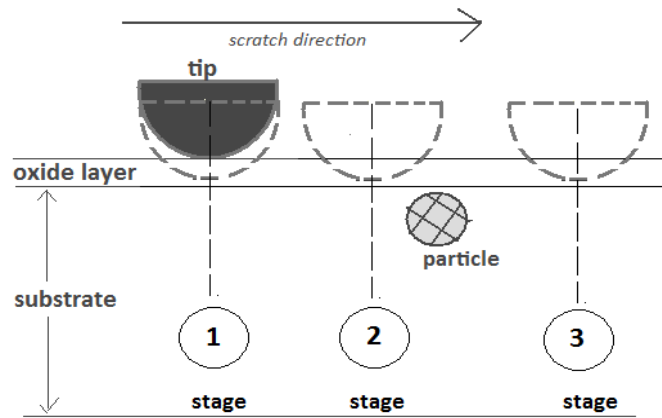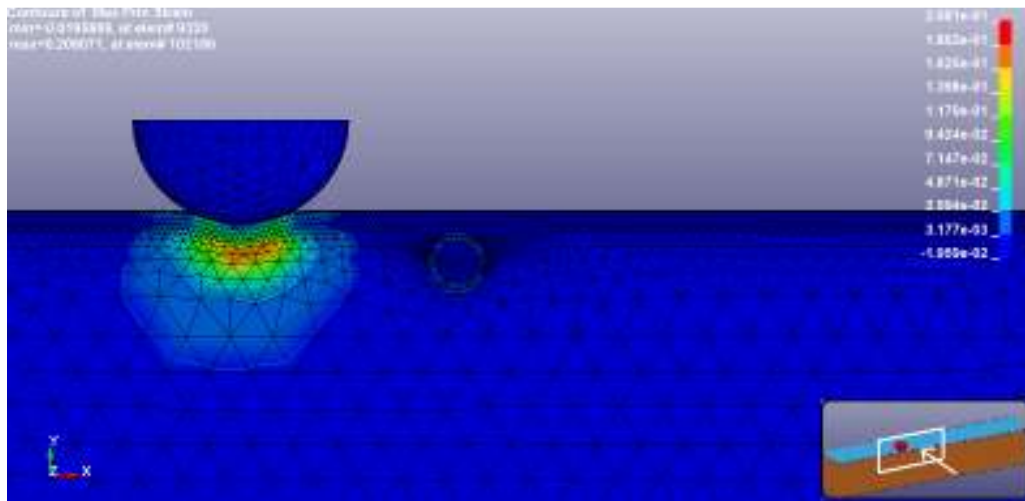Figure 7 and 8 depict the strain contours in the oxide scale and in the substrate at room temperature and high
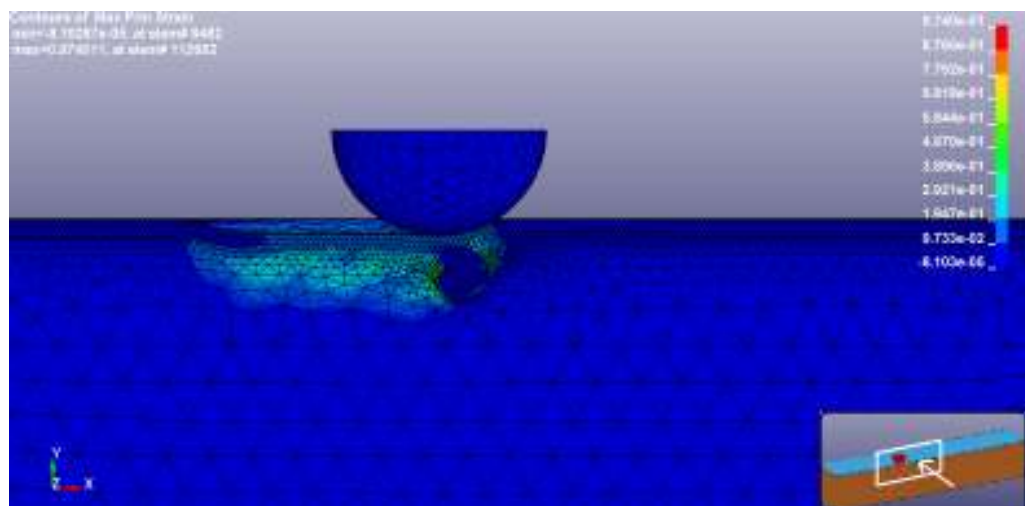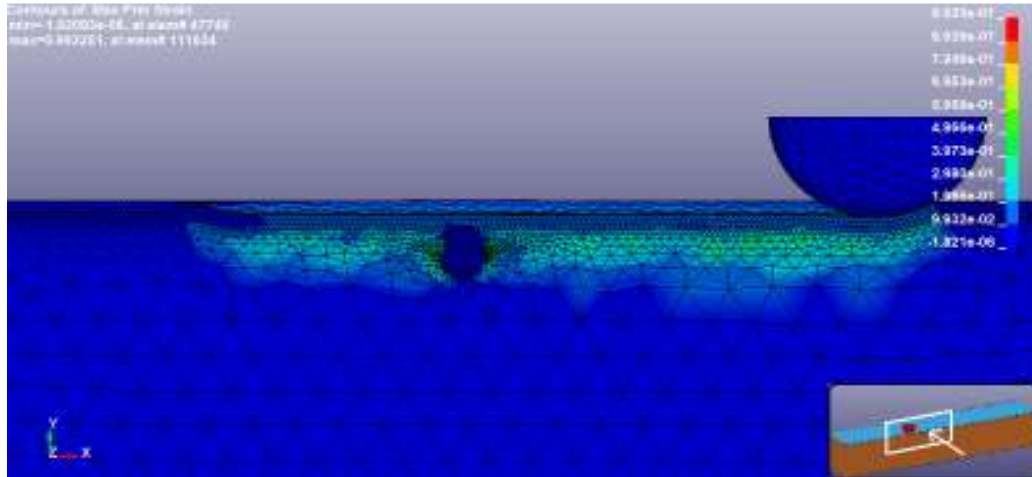

Fig. 6: Particle locations below oxide-substrate interface (Case c)

(a)

(b)

(c)

Fig. 7: The strain field of the particle below oxide-substrate interface (in the substrate) at room temperature; (a) before scratching, (b) during scratching, (c) after scratching
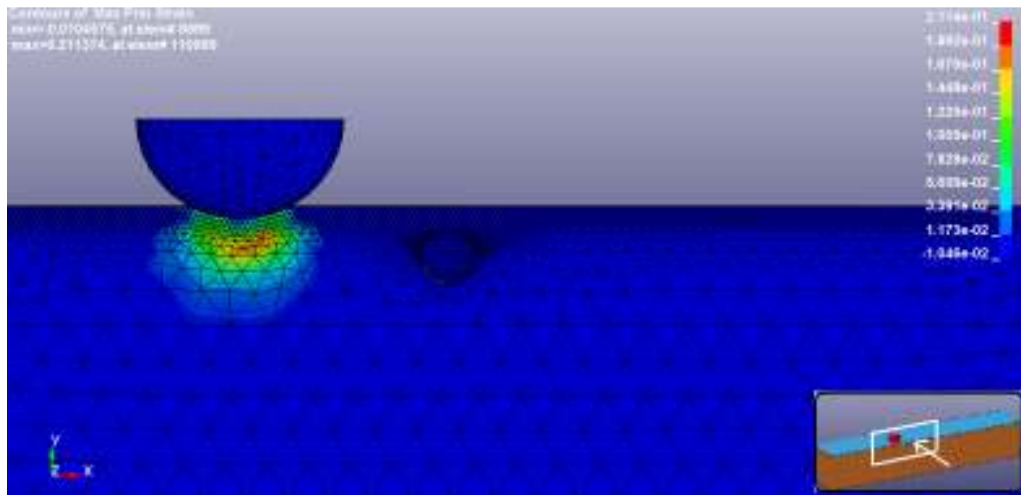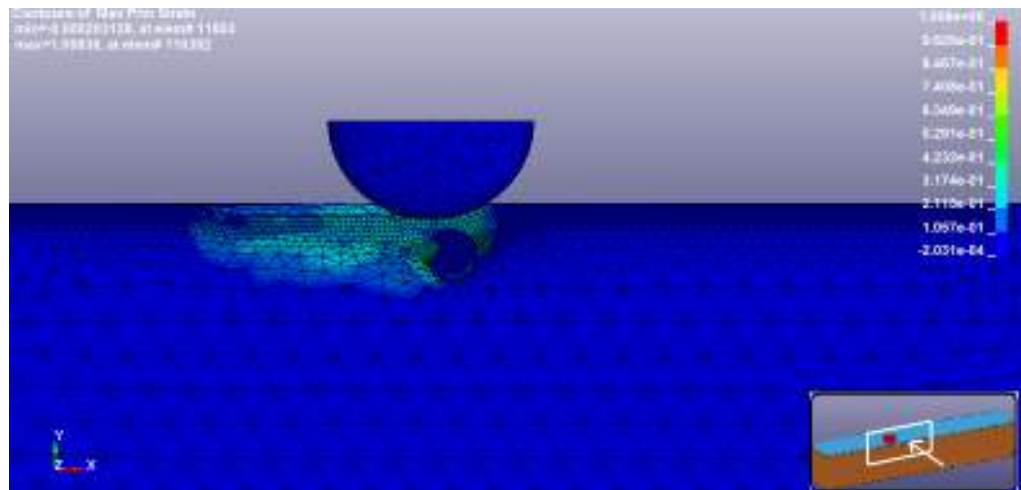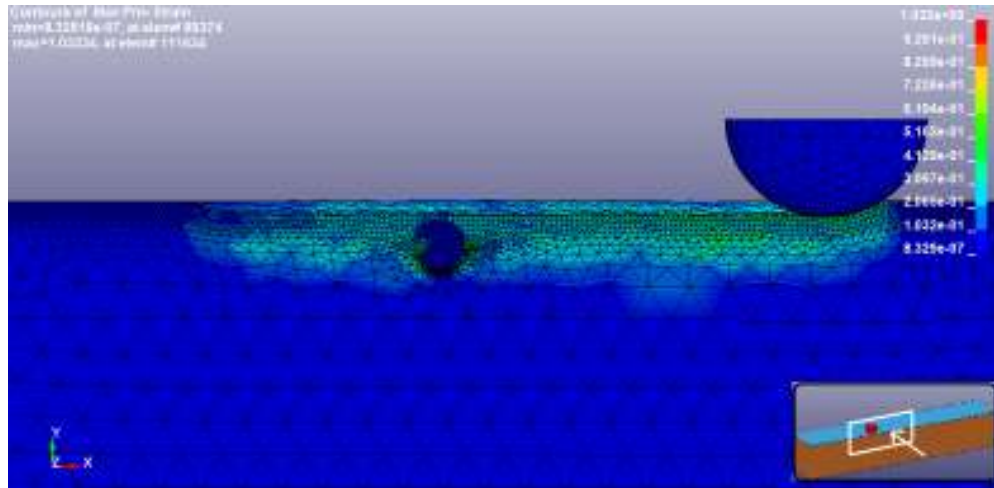

(a)

(b)

(c)

Fig. 8: The strain field of the particle below oxide-substrate interface (in the substrate) at high temperature; (a) before scratching, (b) during scratching, (c) after scratching

Table 3: The summary of maximum strain of particles

	Maximum strain at the stage 2	
	Particle on oxide substrate interface	Particle below oxide-substrate interface (inside the substrate)
Room temperature	1.025	0.97
High temperature	1.076	1.058

temperature respectively. The strain contours below the scratching edge, when the tip moved further into the oxide layer are shown Fig. 7a and 8a. The maximum strain during nanoindentation in both cases was around 0.2.

With further advancement of the tip in the x-direction, the tip would pass the particle without any interaction between the tip and the interface zone of the particle (Fig. 7b and 8b). The interface zone of the particle does not experience any plastic deformation due to scratching in the substrate if the particle is located well below the edge of the scratching, but particles situated immediately below the scratching edge are subjected to plastic deformation when the tip passes over them. Although tip-particle interaction does not happen, the tip movement causes a significant change in strain in the particle and surrounding oxide layer (Fig. 7b and 8b). As a result, the strain increased up to 0.97 and 1.05 at room temperature and high temperature respectively. After leaving the particle region, the strain contours increased slightly up to 0.99 for the room temperature case.

These experiments revealed two positions of the particle which caused them to become embedded into the oxide layer and HSS substrate. The summary of the results is given in Table 3 and Fig. 9. At high temperatures the mechanical properties such as the elastic modulus and yield strength were lower than that of the room temperature case. As a result the strain at high temperature was higher than that at room temperature. This situation was probably due to the

lower yield strength at high temperature being more sensitive to failure. Based on these findings it can be concluded that the high temperature of the work roll would probably increase wear because the increased temperature leads to an increase in the strain, which means there is a high possibility of particle movement to remove and eventually produce delamination of the layer.

Based on this simulation, the particle on oxide-substrate interface and particle in the substrate de-bonded partially which caused the particles to move into the substrate. The results of strain at high temperature are significantly higher than at room temperature, probably due to the difference in the mechanical properties such as the elastic modulus and yield strength of the oxide layer between both cases. The higher elastic modulus and yield strength lead to hardening effect of the oxide layer.

Particles on an oxide free surface became highly de-bonded during interaction between the tip and the particle, so in this case the particle actually represents the debris in the actual case. The way particles are either embedded into or removed from the oxide layer probably depends on the angle of attack of the tip. Yan and Zhang (1994) and Zhang *et al.* (1995) who studied a metal matrix composite MMCs by scratching tests observed pull out of the reinforcement particle and formation of cavities on the scratched surface.

Under normal work roll operations the abrasive factor in the hot strip mill is given by asperities, where

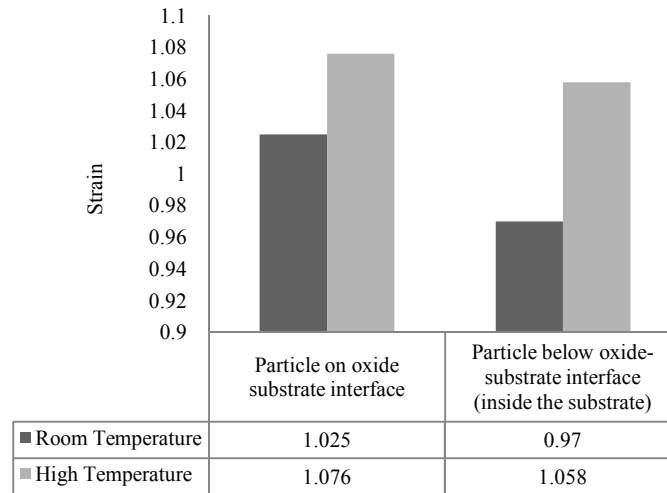|	Particle on oxide substrate interface	Particle below oxide-substrate interface (inside the substrate)
■ Room Temperature	1.025	0.97
■ High Temperature	1.076	1.058

Fig. 9: The strain value of the oxide layer and particle at stage 2

the oxide layers of strips acting as multiple asperities abrade the oxide layers of the work rolls. On the other hand, knowledge about a carbide particle is also important to understand its influences on the abrasive wear. This study describes a comprehensive modelling method of the behaviour of the oxide layer and particles. The particle was 10 μm in diameter. In this analysis the tip is considered to be a rigid body, while the oxide layer, the substrate and the particle must be modelled as a deformable body in order to obtain the necessary deformation formation of the abrasion mechanism.

CONCLUSION

The behaviour of particles and the oxide layer on a high speed steel surface undergoing scratching presents a variety of abrasive phenomena, so a finite element analysis using a physically based oxide scale model is a crucial aspect of this approach. The analysis was used to interpret the wear of the oxide layer formed on the work roll and it also gives a basis for engineering applications. The model of oxide layers was treated as a ductile model. In general, the existence of particles in the oxide layer would increase the wear rate due to the de-bonded particles that contributed to the abrasive factor in the hot strip mills. For example, particles on the oxide-substrate interface have partially de-bonded, which lead to movement of particles.

A comparison of the strain at different temperatures showed that the strain at high temperature $(600^{o}C)$ offered an increase in strain compared to the low temperature case. This increase in temperature can be so significant if it can exceed the transition temperature range, making the interface weaker and giving a high possibility of particle movement. In the FE modelling approach discussed here the tip acted as an asperity that contributes to abrasive wear, whereas in real cases, the abrasive factor in a hot strip mill results from multiple asperities from the oxide layers of strips.

The possibility of abrasion by multiple asperities on the oxide layers of the work rolls is probably higher because of the potential effect of deterioration.

The following conclusions can be drawn based on a finite element modelling of the abrasion mechanism during scratching on the oxide layer formed on HSS work roll and the physical characteristics of the oxide layer and the particles:

- The magnitude and distribution of strains in the oxide layer and interaction of particles with the tip are the main reason for particle de-bonding during scratching.
- The strain at high temperature is higher than at room temperature which leads to a higher sensitivity to failure. Increasing the strain means high probability of particle movement that produces delamination of the layer.
- The strains for particles on the oxide-substrate interface at both temperatures are higher than the particle in the substrate. The interaction between the tip and the particle significantly influences the strains.

REFERENCES

Badisch, E. and C. Mitterer, 2003. Abrasive wear of high speed steels: Influence of abrasive particles and primary carbides on wear resistance. Tribol. Int., 36(10): 765-770.

Boccalini, J.M. and A. Sinatora, 2002. Microstructure and wear resistance of high speed steels for rolling mill rolls. Proceeding of 6th International Tooling Conference, pp: 509-524.

Kang, Y.J., J.C. Oh, H.C. Lee and S. Lee, 2001. Effects of carbon and chromium additions on the wear resistance and surface roughness of cast high-speed steel rolls. Metall. Mater. Trans. A, 32(10): 2515-2525.

Park, J.W., H.C. Lee and S. Lee, 1999. Composition, microstructure, hardness and wear properties of high-speed steel rolls. Metall. Mater. Trans. A, 30(2): 399-409.

Pramanik, A., L.C. Zhang and J.A. Arsecularatne, 2007. An FEM investigation into the behavior of metal matrix composites: Tool-particle interaction during orthogonal cutting. Int. J. Mach. Tool. Manu., 47(10): 1497-1506.

Rodenburg, C. and W.M. Rainforth, 2007. A quantitative analysis of the influence of carbides size distributions on wear behaviour of high-speed steel in dry rolling/sliding contact. Acta Mater., 55(7): 2443-2454.

Vardavoulias, M., 1994. The role of hard second phases in the mild oxidational wear mechanism of high-speed steel-based materials. Wear, 173(1): 105-114.

Yan, C. and L. Zhang, 1994. Single-point scratching of 6061 Al alloy reinforced by different ceramic particles. Appl. Compos. Mater., 1(6): 431-447.

Zamri, W.F.H., P.B. Kosasih, A.K. Tieu, Q. Zhu and H. Zhu, 2012. Variations in the microstructure and mechanical properties of the oxide layer on high speed steel hot rolling work rolls. J. Mater. Process. Tech., 212(12): 2597-2608.

Zamri, W.F.H., P.B. Kosasih, A.K. Tieu, Q. Zhu and H. Zhu, 2013. Finite element modeling of the nanoindentation of layers of porous oxide on high speed steel. Steel Res. Int., 84(12): 1309-1319.

Zhang, Z.F., L.C. Zhang and Y.W. Mai, 1995. Particle effects on friction and wear of aluminium matrix composites. J. Mater. Sci., 30(23): 5999-6004.

Zhu, Q., H.T. Zhu, A.K. Tieu, M. Reid and L.C. Zhang, 2010. In-situ investigation of oxidation behaviour in high-speed steel roll material under dry and humid atmospheres. Corros. Sci., 52(8): 2707-2715.